6-15-2007

A Coupled Remote Sensing and Simplified Surface Energy Balance Approach to Estimate Actual Evapotranspiration from Irrigated Fields

Gabriel B. Senay
South Dakota State University

Michael Budde
SAIC/U.S. Geological Survey EROS

James P. Verdin
SAIC/U.S. Geological Survey EROS

Assefa M. Melesse
Department of Earth and Environment, Florida International University, melessea@fiu.edu

Full Research Paper

A Coupled Remote Sensing and Simplified Surface Energy Balance Approach to Estimate Actual Evapotranspiration from Irrigated Fields

Gabriel B. Senay [1,*], **Michael Budde** [2], **James P. Verdin** [3] **and Assefa M. Melesse** [4]

[1] SAIC, contractor to U.S. Geological Survey (USGS) Center for Earth Resources Observation and Science (EROS)/Geographic Information Science Center of Excellence (GIScCE), South Dakota State University, Sioux Falls, SD, USA. Work performed under USGS contract 03CRCN0001.
E-mail: senay@usgs.gov; Tel: (605) 594-2758

[2] SAIC/U.S. Geological Survey EROS, Sioux Falls, SD, USA. E-mail: mbudde@usgs.gov;
Tel: (605) 594-2619

[3] U.S. Geological Survey EROS, Sioux Falls, SD, USA. E-mail: verdin@usgs.gov;
Tel: (605) 594-6018

[4] Department of Environmental Studies, Florida International University, Miami, FL, USA.
E-mail: assefa.melesse@fiu.edu; Tel: (305) 348-6518

* Author to whom correspondence should be addressed.

Abstract: Accurate crop performance monitoring and production estimation are critical for timely assessment of the food balance of several countries in the world. Since 2001, the Famine Early Warning Systems Network (FEWS NET) has been monitoring crop performance and relative production using satellite-derived data and simulation models in Africa, Central America, and Afghanistan where ground-based monitoring is limited because of a scarcity of weather stations. The commonly used crop monitoring models are based on a crop water-balance algorithm with inputs from satellite-derived rainfall estimates. These models are useful to monitor rainfed agriculture, but they are ineffective for irrigated areas. This study focused on Afghanistan, where over 80 percent of agricultural production comes from irrigated lands. We developed and implemented a Simplified Surface Energy Balance (SSEB) model to monitor and assess the performance of irrigated agriculture in Afghanistan using a combination of 1-km thermal data and 250-m Normalized Difference Vegetation Index (NDVI) data, both from the Moderate

Resolution Imaging Spectroradiometer (MODIS) sensor. We estimated seasonal actual evapotranspiration (ETa) over a period of six years (2000-2005) for two major irrigated river basins in Afghanistan, the Kabul and the Helmand, by analyzing up to 19 cloud-free thermal and NDVI images from each year. These seasonal ETa estimates were used as relative indicators of year-to-year production magnitude differences. The temporal water-use pattern of the two irrigated basins was indicative of the cropping patterns specific to each region. Our results were comparable to field reports and to estimates based on watershed-wide crop water-balance model results. For example, both methods found that the 2003 seasonal ETa was the highest of all six years. The method also captured water management scenarios where a unique year-to-year variability was identified in addition to water-use differences between upstream and downstream basins. A major advantage of the energy-balance approach is that it can be used to quantify spatial extent of irrigated fields and their water-use dynamics without reference to source of water as opposed to a water-balance model which requires knowledge of both the magnitude and temporal distribution of rainfall and irrigation applied to fields.

Keywords: evapotranspiration, energy balance, SSEB, reference ET, irrigation

1. Introduction

As reconstruction efforts in Afghanistan continue, the need for an accounting of the country's water balance is necessary to address current and future water use scenarios. One aspect of the water balance equation involves an assessment of the water demands by irrigated agricultural lands. Since large and widely dispersed populations depend on rainfed and irrigated agriculture and pastoralism, large-area monitoring and forecasting are important inputs to such assessments. The Famine Early Warning Systems Network (FEWS NET), an activity funded by the United States Agency for International Development (USAID), employs a crop water-balance model (based on the water demand and supply at a given location) to monitor the performance of rainfed agriculture and forecast relative production before the end of the crop growing season. Although a crop water-balance approach is effective for monitoring rainfed agriculture [1, 2], irrigated agriculture is best monitored by other methods since the supply (water used for irrigation) is usually generated from upstream areas, which are distant from the demand location.

The surface energy balance method has been successfully applied by several researchers [3-6] to estimate crop water use in irrigated areas. Their approach requires solving the energy balance equation at the surface (Equation 1) where the actual evapotranspiration (ETa) is calculated as the residual of the difference between the net radiation to the surface and losses due to the sensible heat flux (energy used to heat the air) and ground heat flux (energy stored in the soil and vegetation).

$$LE = Rn - G - H \tag{1}$$

LE = Latent heat flux (energy consumed by evapotranspiration) (W/m^2)

Rn = Net radiation at the surface (W/m^2)

G = Ground heat flux (W/ m^2)

H = Sensible heat flux (W/ m^2)

The estimation of each of these terms from remotely sensed imagery requires high quality data sets. Allen et al. [3] described the several steps required to estimate actual ET using the surface energy-balance method that employs the *hot* and *cold* pixel approach of Bastiaanssen et al. [4]. In summary, for the net radiation term, data on incoming and outgoing radiation and the associated surface albedo and emissivity fractions for shortwave and long wave bands are required. The ground heat flux is estimated using surface temperature, albedo, and normalized difference vegetation index (NDVI). The sensible heat flux is estimated as a function of the temperature gradient above the surface, surface roughness, and wind speed.

Although solving the full energy-balance approach has been shown to give good results in many parts of the world, the data and skill requirements to solve for the various terms in the equation are prohibitive for operational applications where year-to-year differences and long term anomalies are more useful than absolute values. In this study, we developed and implemented a simplified version of the surface energy-balance approach to estimate actual ET while maintaining and extending the major assumptions in the Surface Energy Balance Algorithm for Land (SEBAL, Bastiaanssen et al. [4]) and the Mapping Evapotranspiration at High Resolution using Internalized Calibration (METRIC, Allen et al. [3]) method. Both methods assume that the temperature difference between the land surface and the air (near-surface temperature difference) varies linearly with land surface temperature. They derive this relationship based on two anchor pixels known as the *hot* and *cold* pixels, representing dry and bare agricultural fields and wet and well-vegetated fields, respectively. The SEBAL and METRIC methods use the linear relationship between the near-surface temperature difference and the land surface temperature to estimate the sensible heat flux which varies as a function of the near-surface temperature difference, by assuming that the *hot* pixel experiences no latent heat, i.e., ET = 0.0, whereas the *cold* pixel achieves maximum ET. Similarly, Su et al. [7] have developed a Surface Energy Balance System (SEBS) that refers to the *hot* and *cold* extreme conditions as "dry" and "wet", respectively.

In this study, we extended this assumption with a simplification by stating that the latent heat flux (actual evapotranspiration) also varies linearly between the *hot* and *cold* pixels. This assumption is based on the logic that the temperature difference between soil surface and air is linearly related to soil moisture [8]. Furthermore, crop soil water-balance methods estimate actual ET using a linear reduction from the potential ET depending on soil moisture [12, 1]. Therefore, we argue that actual ET can be estimated by the near-surface temperature difference, which in turn is estimated from the land surface temperatures of the *hot* and *cold* pixels in the study area. In other words, while the *hot* pixel of a bare agricultural area experiences little ET and the *cold* pixel of a well-watered irrigated field experiences maximum ET, and the remaining pixels in the study area will experience ET in proportion to their land surface temperature in relation to the *hot* and *cold* pixels. This approach can be compared to the crop water stress index (CWSI) first developed by Jackson [9]. The CWSI is derived from the temperature

difference between the crop canopy and the air. Dividing the current temperature difference (canopy vs air) by known upper and lower canopy air temperature difference values creates a ratio index varying between 0 and 1. The lower limiting canopy temperature is reached when the crop transpires without water shortage, and the upper limiting canopy temperature is reached when the plant transpiration is zero, owing to water shortage, Qiu et al. [10]. In this study, the *cold* and *hot* anchor land surface temperature pixel values are the equivalent of the lower and upper limiting canopy temperatures of the CWSI method.

The main objective of this study was to produce actual evapotranspiration estimates using a combination of a simplified surface energy balance (SSEB) approach and remotely-sensed MODIS thermal imagery and global reference ET over known irrigated fields in Afghanistan.

2. Methods

2.1. Study sites

The study focuses on two major expanses of irrigation in the Helmand and Kabul basins (Figure 1). As mentioned, the water use by irrigated agricultural lands is one aspect of the total water balance in these areas. This work was done as part of a larger Afghanistan water project that identified these two basins as those of primary concern. Because this method relies heavily on temperature variability, each of these areas was further sub-divided into 3 sections of irrigated cropland in order to minimize the effects of elevation differences on surface temperature measures. Table 1 illustrates differences in area and median elevation for each of the sub-divisions. For each sub-division, a polygon was defined around the irrigated fields using a combination of Landsat, Advanced Spaceborne Thermal Emission and Reflection Radiometer (ASTER), and Moderate Resolution Imaging Spectroradiometer (MODIS) data sets. The irrigated areas consist of both well-vegetated and sparsely vegetated areas, with some arid/semi-arid areas at the periphery. In the case of the Helmand basin, Helmand 1 is comprised of the area upstream of Lashkar Gah, Helmand 2 is an approximately 35km stretch of irrigated land south of Lashkar Gah along the main river channel, and Helmand 3 is the remainder of the irrigated area along the channel extending to the south and west. The Kabul basin sub-divisions consist of an extensive irrigated area north of Kabul and a narrower band of irrigation along the river south and west of Kabul. The latter area, Kabul 2, is adjacent to one of the primary stream channels feeding the city and could have significant impacts on municipal water supply. Kabul 1 and Kabul 3 include the large area of irrigated agriculture that is found near the headwaters of the Panjir River. Wheat is the primary cultivated crop in all areas.
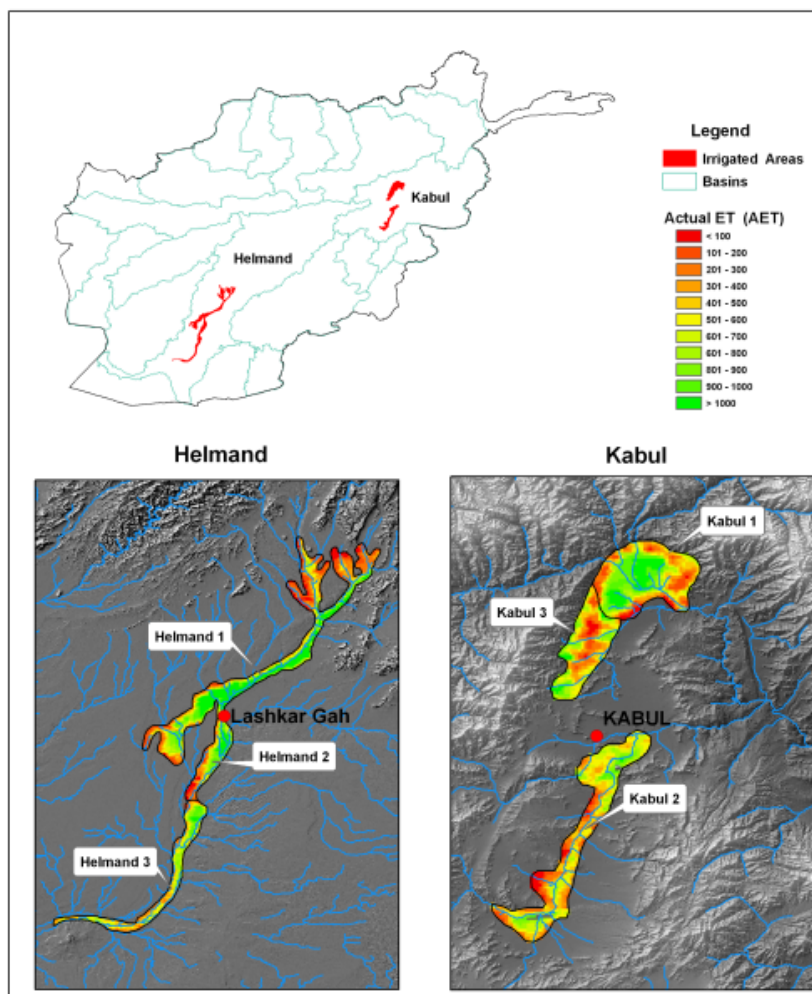
Figure 1. Study sites showing the irrigated fields in the Helmand and Kabul drainage basins. Enlarged windows illustrate the three sub-divisions within each irrigated area and their relation to stream networks.

Table 1. Study area characteristics by irrigation area sub-division.

Sub-Division	Area (sq km)	Median Elevation (m)
Kabul 1	741	1508
Kabul 2	864	1896
Kabul 3	448	1671
Helmand 1	2120	860
Helmand 2	429	746
Helmand 3	719	673

2.2. Data Set Characteristics

The primary data sets for this study were derived from the MODIS sensor flown onboard the Terra satellite. MODIS Land Surface Temperature (LST) data were used to calculate the crucial

evapotranspiration (ET) fractions explained in the procedures section of this manuscript. Additionally, MODIS NDVI data were used for irrigated area delineation and identifying highly-vegetated versus sparsely vegetated areas within the agricultural zone. The global reference ET data were obtained from the archives of USGS/FEWS NET operational model outputs. Each data set is further described below.

MODIS Land Surface Temperature: Thermal surface measurements were collected from the MODIS 8-day Land Surface Temperature/Emissivity (LST/E) product (MOD11A2). The MODIS instrument provides 36 spectral bands, including 16 in the thermal portion of the spectrum. The LST/E images provide per-pixel temperature and emissivity values at 1-km spatial resolution for the 8-day composite product. Temperatures are extracted in degrees Kelvin with a view-angle dependent algorithm applied to direct observations. This study utilized average daytime land surface temperature measurements for 8-day composite periods throughout the growing season (Figure 2). More than twenty five 8-day periods beginning in early April through the end of October were processed. Table 2 shows the MODIS day of year representing the first day of the 8-day MODIS LST composite period and corresponding calendar dates for all years.

Table 2. MODIS composite day and corresponding calendar dates.

MODIS Composite Day	2001, 2002, 2003, 2005	2000, 2004
89	Mar 30 - Apr 06	Mar 29 - Apr 05
97	Apr 07 - 14	Apr 06 - 13
105	Apr 15 - 22	Apr 14 - 21
113	Apr 23 - 30	Apr 22 - 29
121	May 01 - 08	Apr 30 - May 07
129	May 09 - 16	May 08 - 15
137	May 17 - 24	May 16 - 23
145	May 25- Jun 01	May 24 - 31
153	Jun 02 – 09	Jun 1 - 08
161	Jun 10 – 17	Jun 09 - 16
169	Jun 18 – 25	Jun 17 - 24
177	Jun 26 - Jul 03	Jun 25 - Jul 02
185	Jul 04 - 11	Jul 03 - 10
193	Jul 12 - 19	Jul 11 - 18
201	Jul 20 - 27	Jul 19 - 26
209	Jul 28 - Aug 04	Jul 27 - Aug 03
217	Aug 05 - 12	Aug 04 - 11
225	Aug 13 - 20	Aug 12 - 19
233	Aug 21 - 28	Aug 20 - 27

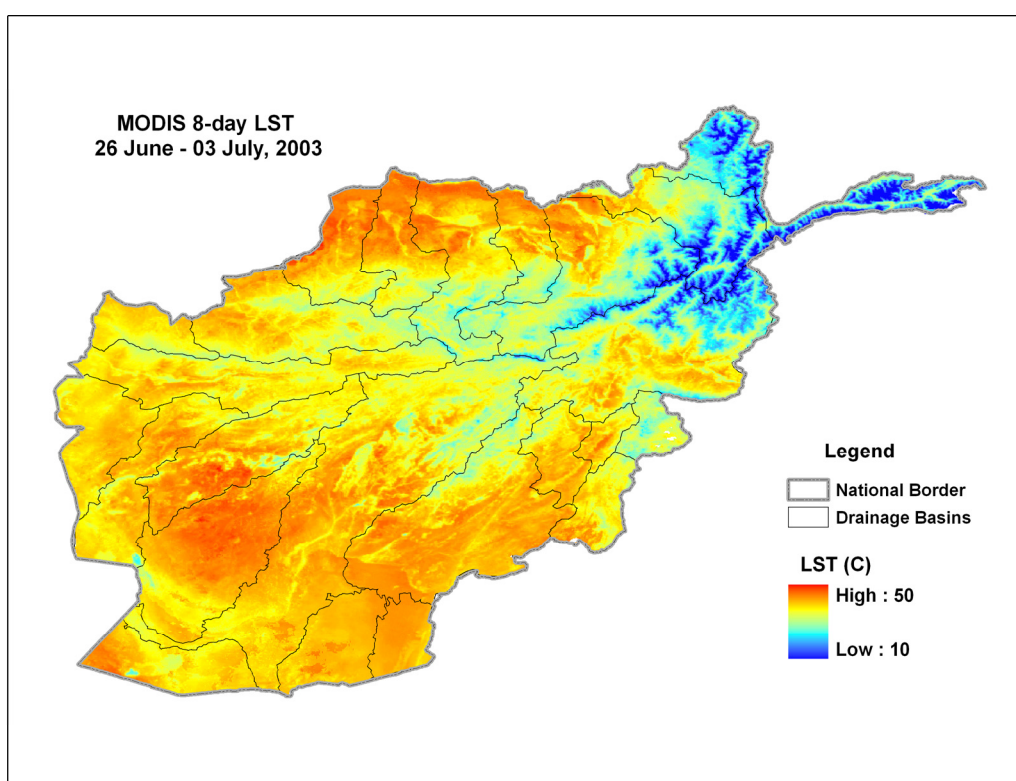| 241	Aug 29 - Sep 05	Aug 28 - Sep 04
249	Sep 6 - 13	Sep 05 - 12
257	Sep 14 - 21	Sep 13 - 20
265	Sep 22 - 29	Sep 21 - 28
273	Sep 30 - Oct 07	Sep 29 – Oct 06
281	Oct 08 - 15	Oct 07 – 14
289	Oct 16 - 23	Oct 15 – 22
297	Oct 24 - 31	Oct 23 – 30

Figure 2. An 8-day composite of MODIS Land Surface Temperature (LST, ^{o}C) in late June/early July 2003.

MODIS Vegetation Index: MODIS Vegetation Index (VI) products use reflectance measures in the red (620 – 670 nm), near infrared (841 – 876 nm), and blue (459 – 479 nm) bands to provide spectral measures of vegetation vigor. The MODIS VI products include the standard normalized difference vegetation index (NDVI) and the enhanced vegetation index (EVI). Both indices are available at 250-m, 500-m, and 1-km spatial resolution. The primary difference between the two indices is that EVI uses blue reflectance to provide better sensitivity in high biomass regions. Because this study was concentrated on irrigated agriculture in an otherwise dry land environment, we used the standard 16-day NDVI product at 250-m resolution for this analysis (Figure 3).

The MODIS vegetation index and land surface temperature data are distributed, at no cost, by the Land Processes Distributed Active Archive Center (LPDAAC), located at the USGS Center for Earth Resources Observation and Science (EROS) Center (http://LPDAAC.usgs.gov).
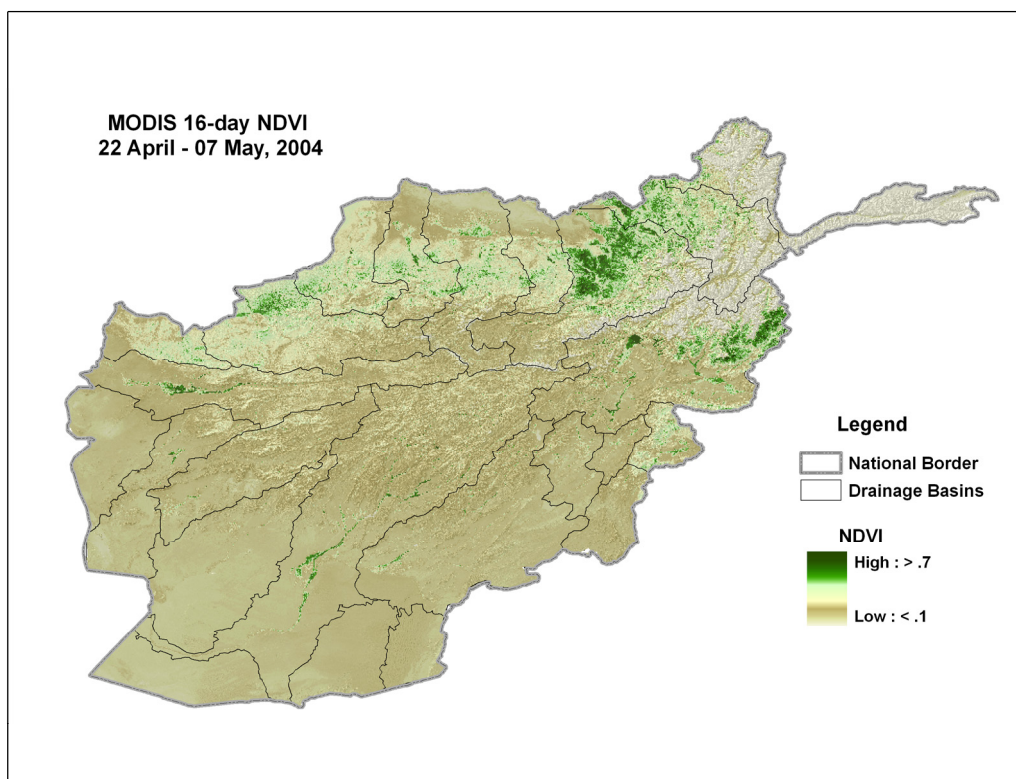

Figure 3. MODIS 250m 16-day NDVI composite in late April/early May 2004.

Reference ET: The global 1-degree reference ET (ETo), based on the 6-hourly Global Data Assimilation Systems (GDAS) model output, is calculated daily at EROS (Senay and Verdin [11]). The GDAS ETo (Figure 4) uses the standard Penman-Monteith equation as outlined in the FAO publication for short-grass ETo by Allen et al. [12]. The feasibility of using the GDAS ETo for such applications was recommended by Senay and Verdin [11] after a comparison with station-based daily ETo showed encouraging results with r^2 values exceeding 0.90. Daily global ETo values were available for all days between 2001 and 2005. For 2000, the daily ETo values were not complete. For the missing time periods, the average daily ETo from 2001 to 2005 was used.

Prior to using these data for our analysis, a downscaling of the GDAS 1-degree data was performed to produce a 10-km GDAS ETo. The approach utilized the International Water Management Institute (IWMI) historical (1961-90) potential evapotranspiration (PET). The IWMI data set is based on data originally compiled at 16-km spatial resolution that has been disaggregated to 10-km. The downscaling technique utilized the 10-km historical IWMI PET data to create a fractional relationship, on a per pixel basis, between each 10-km IWMI pixel (x) and the corresponding 100-km IWMI pixel (y) value (artificially created to simulate the 100-km GDAS). This fractional relationship was then applied back to the 100-km GDAS pixels to downscale these data to a spatial resolution of 10-km (Equation 2). The resulting 10-km ETo grids were used in this analysis (Figure 4). The downscaling method was developed and validated by the authors using similar IWMI data to develop the fractions

over the conterminous US and the results compared favorably with station-based ETo in California. Thus, the method was proven to be an effective technique to downscale the Global GDAS ETo. A manuscript is being prepared to publish the validation of the downscaling technique.

$$x / y * \text{GDAS ETo} \tag{2}$$

Where, "x" represents 10-km IWMI PET and "y" is the 100-km IWMI PET

2.3. Procedures/Analysis

Sets of three *hot* and three *cold* pixels were selected for each 8-day composite period for each year of growing season data. An average of the 3 pixels was used to represent the *hot* and *cold* values in each of the six study areas. The study area was divided into 6 irrigation areas to reduce elevation differences that are large enough to cause land surface temperature differences since the premise of the existing model is based on the assumption that surface temperature differences are only caused by differences in moisture availability and water use. For a given time period, cold pixels, representing well vegetated and well watered crops, were selected based on a combination of low LST values and high values in the MODIS NDVI. Similarly, hot pixels, representing low density vegetation and relatively dry land, were identified by high LST values and very low NDVI values.

Land surface temperature values for each of the six pixels (3 *hot*, 3 *cold*) were extracted using ArcGIS 9.0 software [13]. The resulting database files were imported into an Excel spreadsheet where average *hot* and *cold* pixel values were calculated.
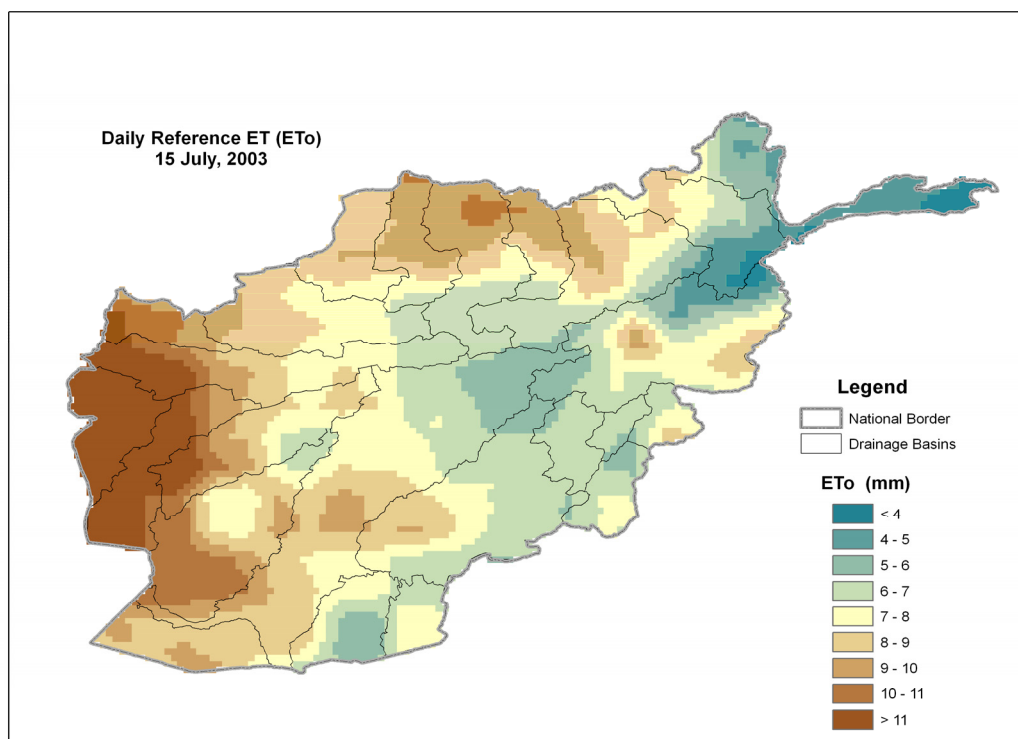

Figure 4. Daily GDAS reference ET (ETo) at 10km resolution, downscaled from 1 degree resolution using the IWMI long-term average gridded ETo.

With the assumption that *hot* pixels experience very little ET and *cold* pixels represent maximum ET throughout the study area, the average temperature of *hot* and *cold* pixels could be used to calculate proportional fractions of ET on a per pixel basis. The ET fraction (ET_f) was calculated for each pixel by applying the following equation (Equation 3) to each of the 8-day MODIS land surface temperature grids.

$$ET_f = \frac{TH - Tx}{TH - TC} \qquad (3)$$

where TH is the average of the three *hot* pixels selected for a given scene; TC is the average of the three *cold* pixels selected for that scene; and Tx is the land surface temperature value for any pixel in the composite scene.

The ET_f equation was applied to each 8-day average composite for each year, resulting in a series of more than 25 images per season. The images contained ET fractions for each pixel that were used to estimate actual ET throughout the growing season.

The ET_f is used in conjunction with ETo to calculate the per pixel actual ET (ETa) values in a given scene (Equation 4). The calculation procedure is similar to the use of a crop coefficient (Kc) and soil stress coefficient (Ks) in crop water-balance-based ET modeling where a ETo is adjusted in a multiplicative manner using Kc that is dependent on crop type and stage, and Ks which is dependent on soil moisture [1]. Daily ETo values were used to create average 8-day ETo corresponding to the LST composite periods.

$$Eta = ET_f * ETo \qquad (4)$$

This simplified approach in SSEB allowed us to use modeled ETo at a coarse spatial resolution to derive spatially distributed high-resolution ETa values based on land surface temperature variability at 1-km resolution. Knowledge of ETa at a higher spatial resolution during the growing season provides important insight into the extent of irrigated cropland, the quality of the growing season, and associated seasonal water use.

Preliminary validation of the performance of SSEB was undertaken using crop fields in the north central United States. Corn and soybean fields in two South Dakota counties, Brookings and Moody, were used to compare model results with the SEBAL and METRIC methods. Landsat thermal scenes from August 1, 2000 and August 4, 2001 were used to assess the performance of the simplified energy balance method (SSEB). Depending on the crop type and year, the correlation coefficient (R^2) between SSEB and METRIC varied from 0.94 to 0.99 and with SEBAL from 0.55 to 0.79 (unpublished work by Swanson and Trooien, 2007, personal communication). A sample scatter plot of the validation work between SSEB and METRIC is shown in Figure 5.

The lack of field data in Afghanistan precludes a quantitative validation of the results in an absolute manner. However, quantitative analysis of the findings can be made by studying the year-to-year variability in relative terms. To this effect, actual crop ET for the six-year period, 2000 – 2005, was

used to assess the quality of each growing season in the Helmand and Kabul study areas. Using masks of the irrigated crop area, described earlier in Figure 1, we used the 1-km gridded actual ET values to calculate spatially averaged actual ET for each season. The results and implications of these comparisons are outlined in detail in the following section.
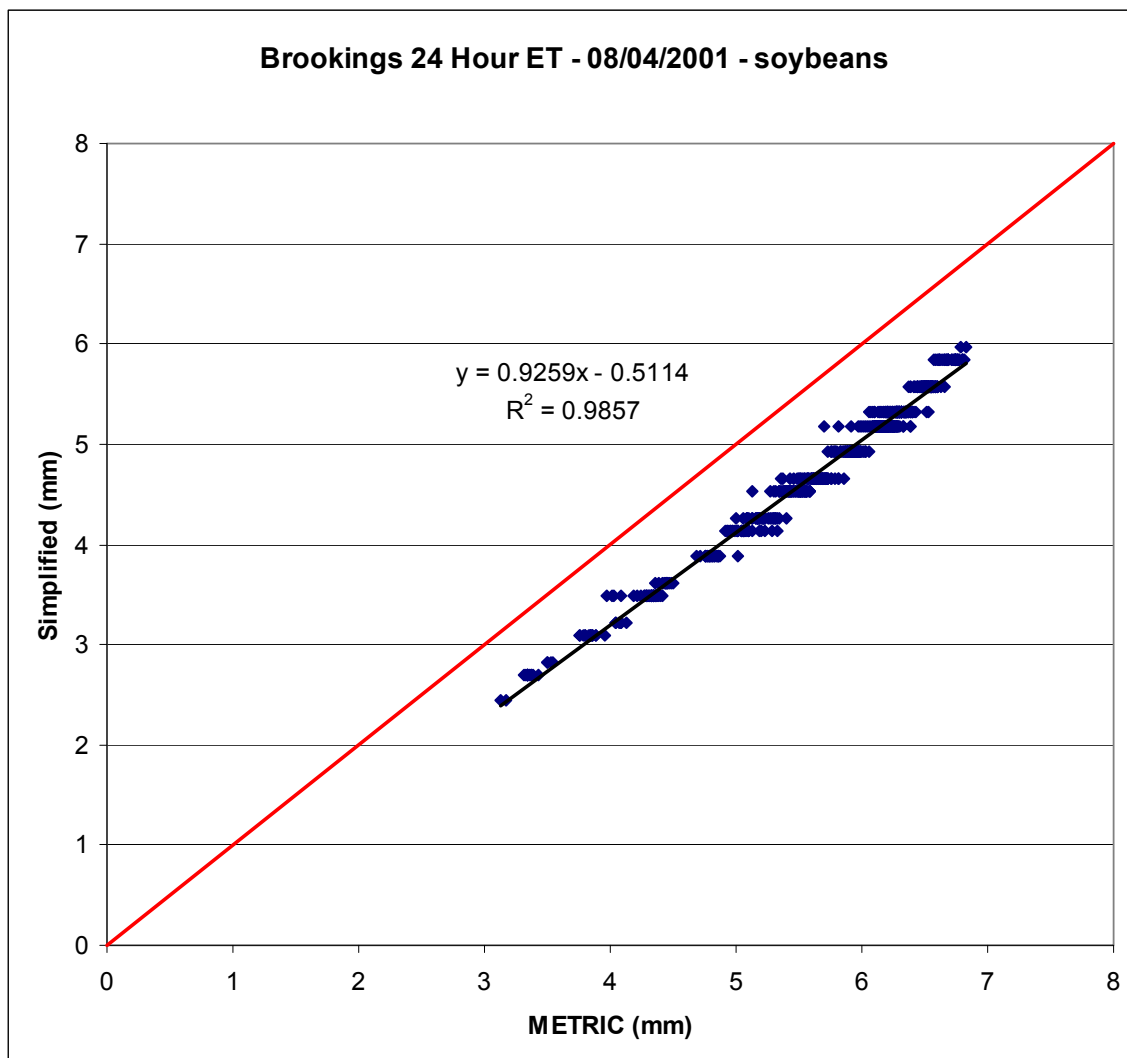

Figure 5. Scatter plot of one-day total actual ET (ETa) estimate between SSEB and METRIC model outputs in a soybean field on August 4, 2001. (Source: Swanson and Trooien, 2007)

3. Results and Discussion

The presentation of results is divided into three primary sections. First, we provide a detailed discussion of the Kabul 1 area (Figure 1). Second, we will discuss in more general terms, the findings for all six study areas. Third, we will elaborate on further analysis that will be needed to provide a more comprehensive assessment of the seasonal irrigated crop demands throughout the Helmand and Kabul drainage basins.

3.1. Kabul 1

A time series of *hot* and *cold* pixel values for each 8-day time period in 2003 is shown in Figure 6. Similar temporal patterns were also observed in other years. For 2003, the *hot* and *cold* pixels were separated by an average of approximately 13 °C throughout the season between May and September. Furthermore, they appeared to increase or decrease in the same direction by about the same magnitude during the peak portions of the crop growing season. However, this separation approaches nearly to 0.0 °C during the off-seasons, particularly close to the start of the season. We believe the existence of such temporal patterns between the *hot* and *cold* pixels is potentially useful in detecting time of start of season for crop monitoring activities. However, early comparisons with seasonal NDVI time series indicate that the period of maximum water use corresponds more with atmospheric demand than with time of maximum vegetative stage, as measured using NDVI (Figure 7). Figure 6 also shows the boundary (extreme) conditions for surface temperature distribution in the study site.
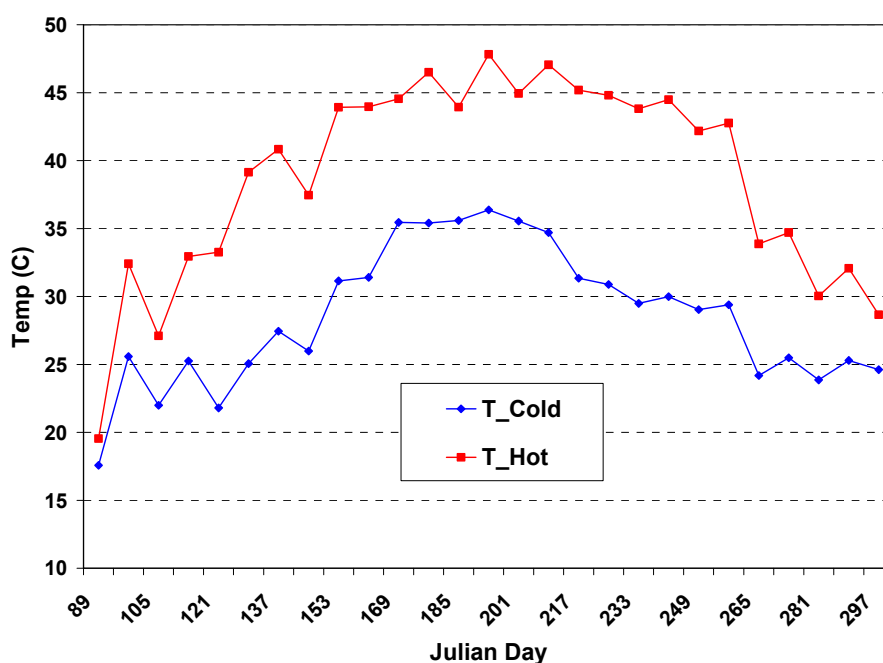

Figure 6. Temporal variation of the *hot* (T_hot) and *cold* (T_cold) pixel values during the 2003 crop growing season in °C.

By properly selecting the extreme temperature areas representing the *hot* (dry/bare) and the *cold* (wet/vegetated) land areas, the remaining pixels in the study area will fall in between these temperature values. The two extreme temperatures also correspond with extremes in ET values. The range of these values varies from zero ETa for the *hot* and dry areas to a high ETa, comparable in magnitude to ETo, for the *cold* and wet areas [3]. In this study, we extended this assumption to include the remaining pixels by suggesting that pixels having land surface temperature values in between these extremes will experience an ET value in direct proportion to the ET fraction as shown in equation 3.
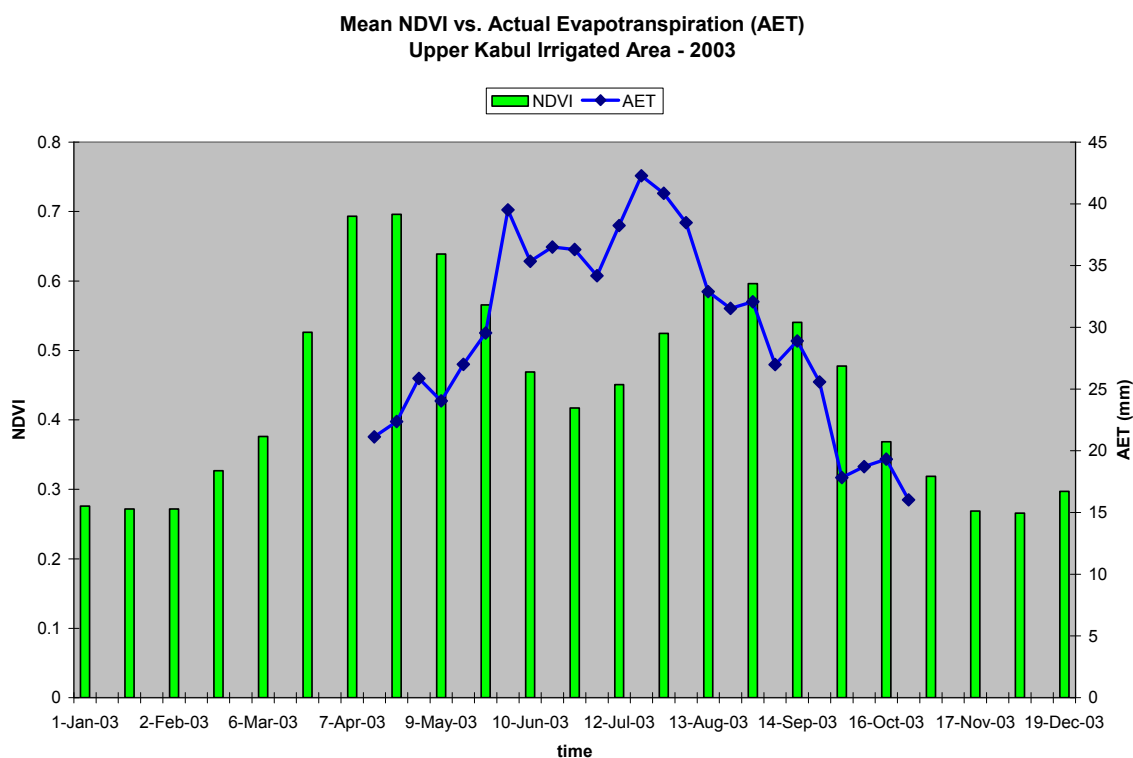
Mean NDVI vs. Actual Evapotranspiration (AET)
Upper Kabul Irrigated Area - 2003

Figure 7. Temporal comparison of spatially averaged 16-day NDVI and 8-day ETa (AET) during the 2003 season.

Figure 8 shows the temporal trend of irrigation water use during the peak growing season for each of the 6 years used in this study. All years show a marked increase in seasonal water use in the late May and early June, a time when both air temperature and atmospheric demand are on the increase. The figure also shows a high level of inter-annual variability in seasonal water use, especially during the month of June. This could be explained by the fact that some crop fields may be taking advantage of spring rainfall and others are being harvested. Also, it may be that variability in spring rainfall could affect the timing and magnitude of seasonal snow melt, causing varying amounts of water to be available for irrigation use on different years. It should also be noted that the vegetation index temporal pattern identified in Figure 7 illustrates that this area is bimodal in its seasonality. Although Figure 7 shows only 2003 growing season NDVI, the bimodal pattern is seen throughout the six-year time series. The high degree of inter-annual variability seen in June is not evident later in the time series because irrigation water is not supplemented by other means. However, the 2003 growing season shows a distinct difference in irrigation water use compared to the other years. The irrigation water use from mid-July to early-August 2003 was 25 percent greater than the average. These findings corroborate field reports of an extensive second season crop during the 2003 growing season. All years showed a downward trend in water use beginning in the middle of August and progressing through September. This would correspond with a time when temperatures become milder and the difference between hot and cold pixels decreases.
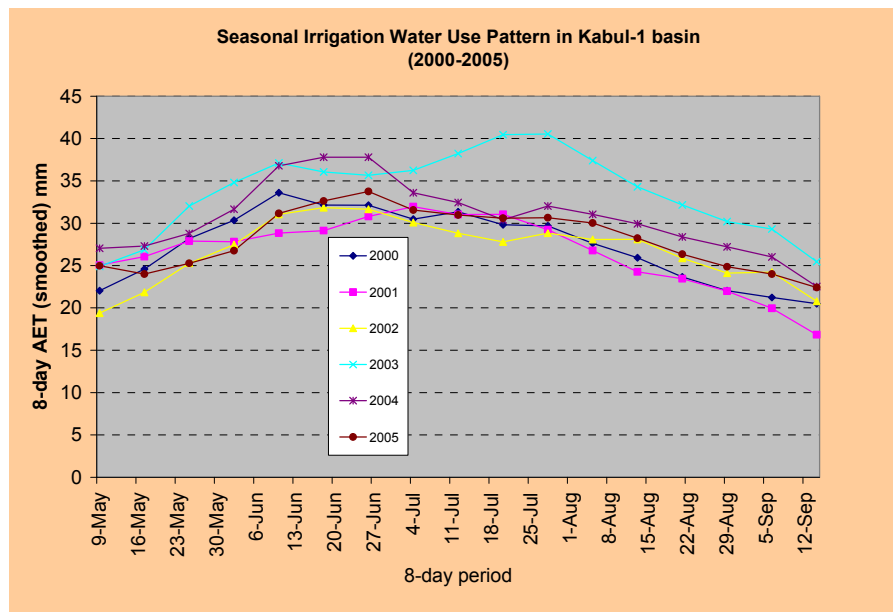
Figure 8. Temporal patterns of seasonal irrigation water use (ETa (AET)) in Kabul 1 for 2000 - 2005. Data is smoothed using a 3-period moving window.

Although the time series raises interesting questions about the temporal variability of water use patterns in the study area, an annual accounting of the irrigated water demand can be met by calculating the total seasonal ETa for each year. The actual crop evapotranspiration is estimated from the product of ET fraction and the ETo as shown by equation 4. Figure 8 shows the temporal patterns of the actual crop ET for each 8-day period. Each data point represents an 8-day actual ET estimate that is spatially averaged over the study area. The spatially-averaged seasonal ETa magnitudes are presented in Figure 9 to illustrate the year-to-year variability in actual ET.
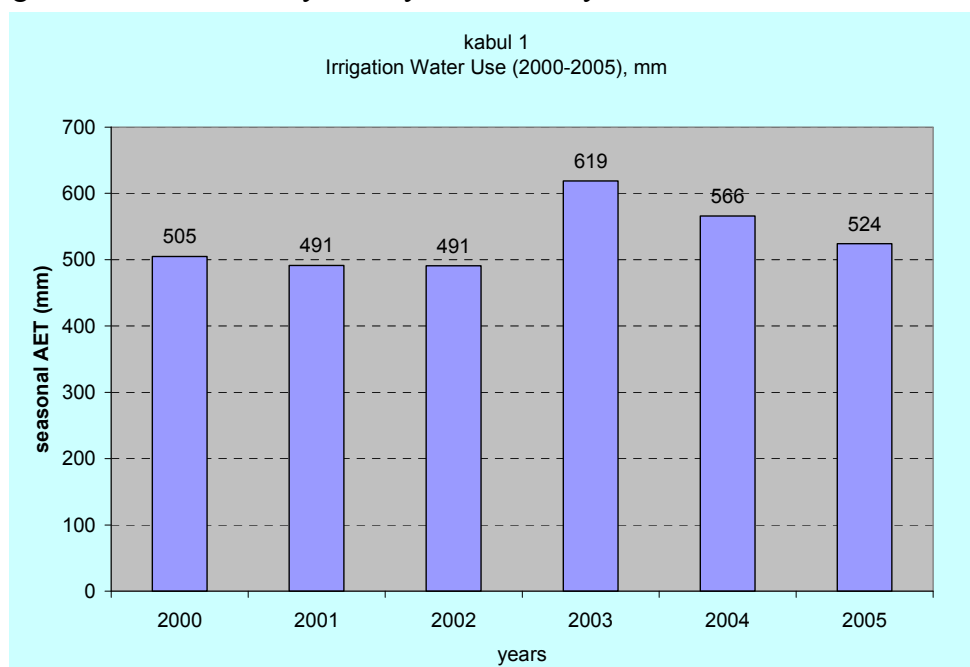

Figure 9. Spatially averaged peak-season (May – Sept.) actual crop ETa (AET) (mm) from 2000-2005.

Figure 9 highlights the fact that 2003 was the best agricultural season during the 5-year period, which is supported by several field reports that the cycle of three consecutive drought years, between 2000 and 2002, was alleviated by good precipitation in the 2003 season. These results are comparable to those from a watershed-based analysis of an operational FEWS NET irrigation supply and demand model, showing that 2002 and 2004 were below an average supply and the 2003 irrigation water supply met the average demand, defined using a 30-year rainfall climatology from 1961 to 1990 **(www.cgiar.org/iwmi/WAtlas/atlas.htm)**. The spatially averaged seasonal ETa for 2003 is approximately 20 percent above the average of the other five years.

While Figures 7 to 9 show spatially-averaged ETa, and Figure 10 presents the spatial variation of the seasonal actual ET in Kabul 1 for all six years. As is shown in Figure 9, the higher values of the 2003 seasonal ET are illustrated by the larger extent of high actual ET classes (darker green colors) compared to other years. Similar patterns of vegetation greenness for the corresponding years were observed from MODIS seasonal maximum NDVI data. The reduction in actual ET values, in all years except 2003, has mainly occurred between two stream segments toward the southwest edge of the irrigated fields in Kabul 1, where a short tributary originates from a much lower elevation than the main stem to the north. The geographic area where lower actual ET values were observed seems to suggest that irrigators/fields further away from the major tributaries would have access to water only if there was a surplus in excess of the demands of the near-stream users. This is in line with a common practice in regions where water rights are not well established or regulated. Furthermore, Figure 10 suggests the possibility of using this method of analysis to estimate harvested irrigated areas for a given year based on a threshold of actual ET required for successful crop growth. For example, in the study area where certain fields consumed up to 800 mm in about 5 months, areas that only used half (400 mm) of the water demanded by a well-watered crop could be considered as unsuccessful and removed from harvested irrigated areas [1, 15]. Although the accuracy of the magnitudes of the estimated actual ET values requires field validation using other methods or field studies, the method's relative performance in terms of capturing the year-to-year variability suggests that the technique has a potential to characterize irrigated field crop performance in relative terms on reasonably homogeneous flat irrigated fields.

The next step in quantifying seasonal water use by irrigated crop land is to convert the ETa values into a volumetric assessment of water use. The method for doing this relies on the ability to calculate an irrigated basin area. Once the irrigated area is determined, the ETa values can be converted to a cubic measure of volumetric ETa. Figure 11 shows 8-day volumetric ETa values averaged over all six years of the study for May through September in Kabul 1. The result is a time series that allows for the assessment of temporal trends in volumetric water use as well as a quantification of seasonal volumetric water use throughout the basin. Preliminary calculations identify June as the month of highest volumetric water use and estimate average seasonal water use to be approximately 294 million cubic meters in Kabul 1. A full accounting of water use for the Kabul basin will require additional work as outlined in the further analysis section.
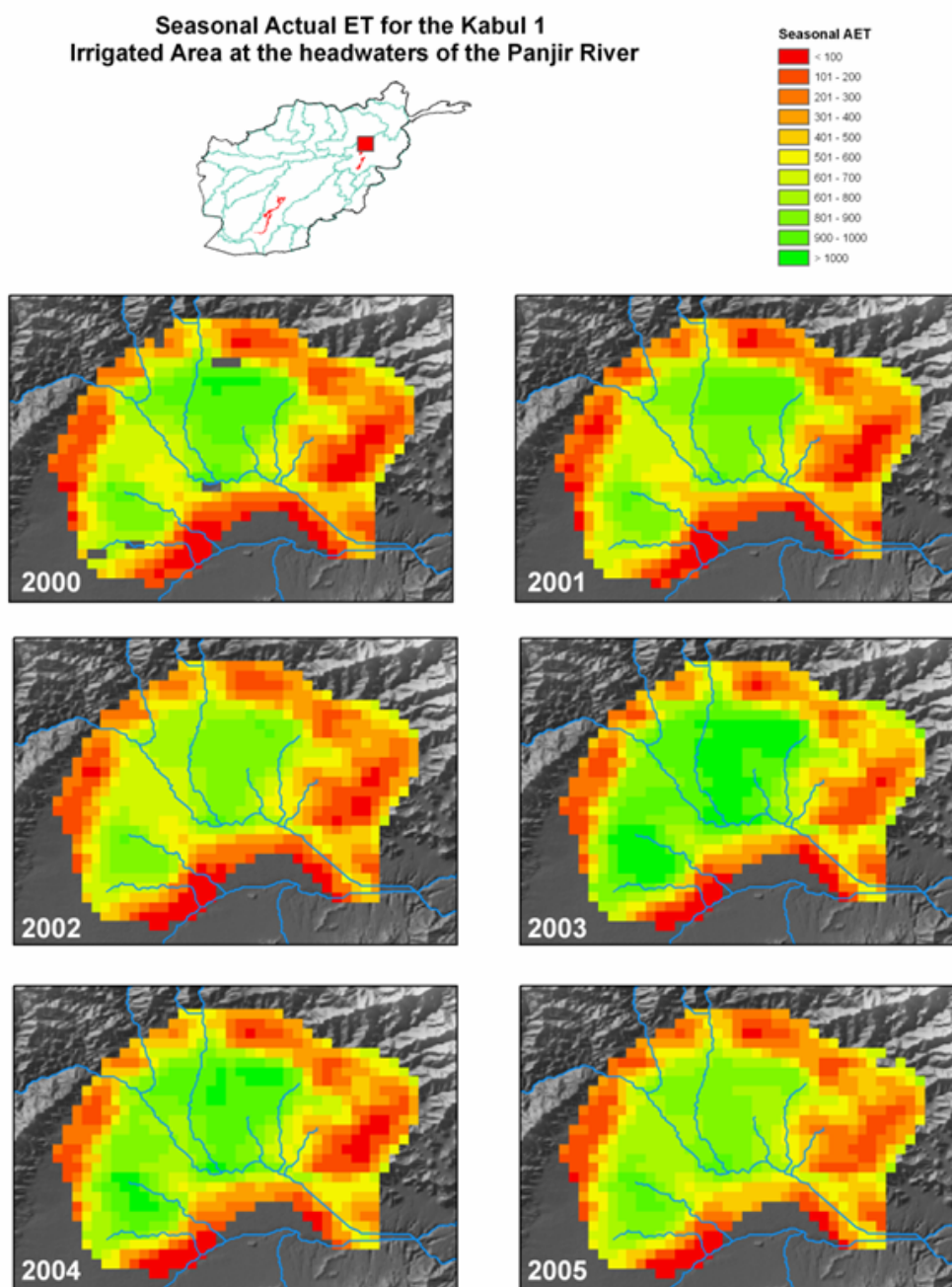
Figure 10. Seasonal (May – Sept.) actual ET (mm) distribution in irrigated fields of the Kabul 1 study area.
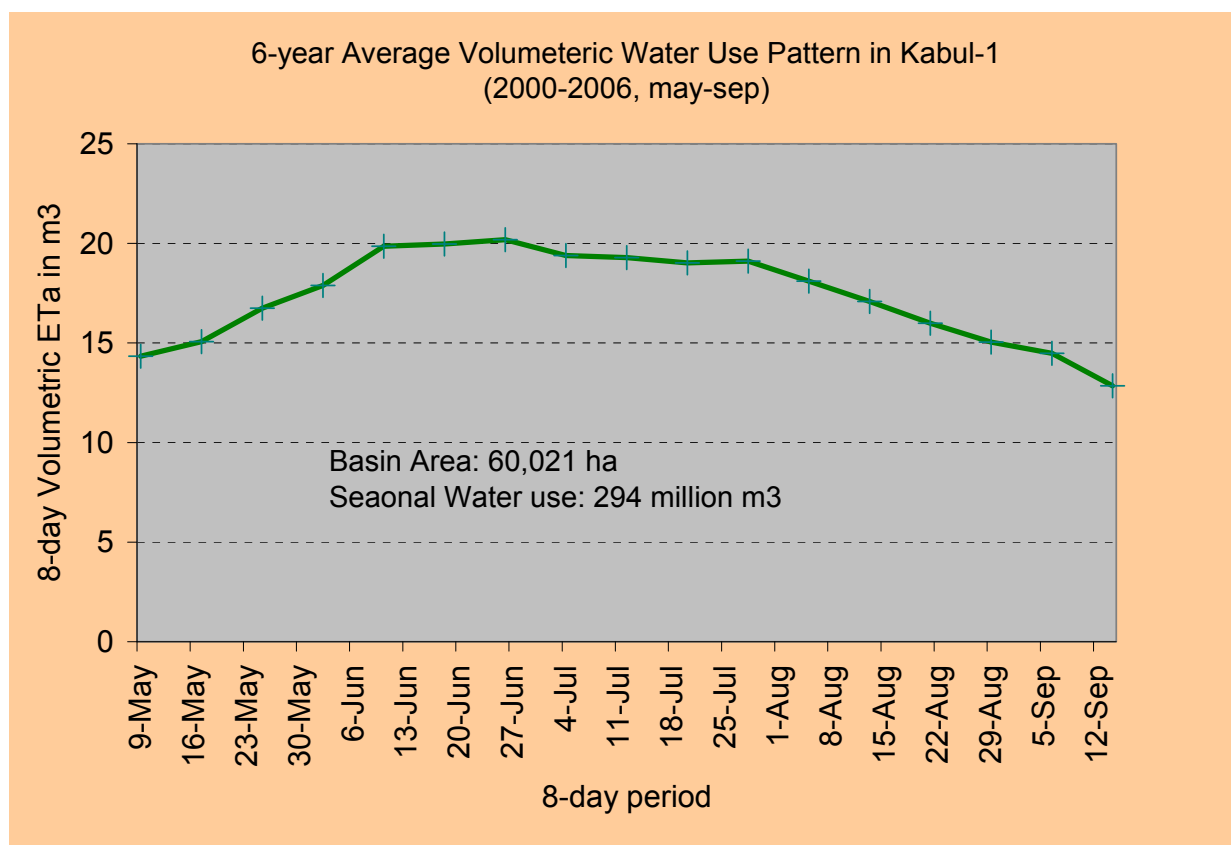
Figure 11. Estimated volumetric water use (ETa, m^3) pattern for the Kabul 1 irrigated area.

3.2. Other Study Areas

Similar detailed assessment of irrigated crop water use has been done for the other five basin sub-divisions. The graph shown in Figure 12 illustrates some of the similarities and differences in the findings for the other study sites. The most common feature among all areas is that the 2003 growing season stands out as having the highest seasonal ETa. Seasonal ETa of nearly 500 mm or greater was found for all study sites during the 2003 growing season. By contrast, almost every other year contained only one or two areas above 500 mm in seasonal ETa. Another characteristic among the six study sites was the high degree of inter-annual variability in seasonal ETa. However, the magnitude of this variability seems to show some regional differences. The Helmand basin areas appear to vary more dramatically than those in the Kabul basin. This seems to be somewhat counter-intuitive due to the fact that the upstream area of the Helmand basin contains the Kajaki Reservoir, which would be expected to provide a regulated release of water downstream. However, many of the irrigated areas of the Helmand stretch far beyond the source of irrigation water and therefore could be impacted by exploitation of water resources further upstream. As mentioned earlier, without proper regulations on water use and stream flow management, those irrigators nearer to the source may benefit the most while those further downstream are adequately supplied only in years of abundant water availability. Another possible explanation for the higher degree of variability in the Helmand region may be the result of crop rotation or fallow. A closer look at the Helmand 3 seasonal ETa (Figure 12) shows a fairly regular pattern of lower (300 – 400 mm) followed the next year by higher ETa (400 – 500 mm).

It could be that some farmers in the region have fields that lay fallow every other year and therefore do not contribute to the seasonal ETa and consequently use less water on an inter-annual basis. Regional crop production reports may be able to provide additional insight into such cropping practices.
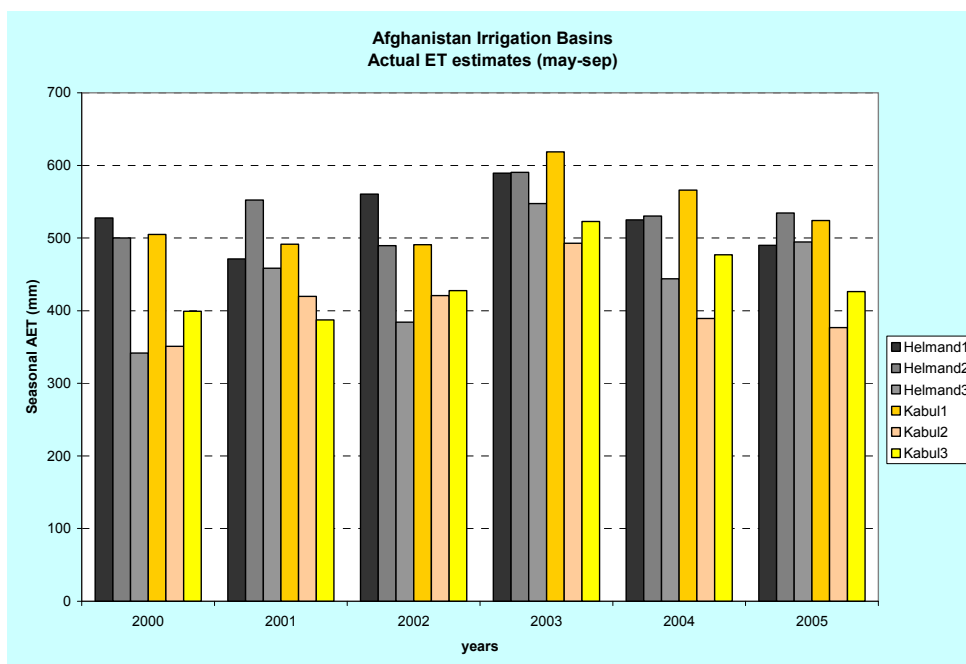

Figure 12. Seasonal ETa (AET) (mm) estimates (2000 – 2005) for all major irrigated areas in the Helmand and Kabul basins.

Table 3. Relative water use changes in the three irrigation areas of Helmand basin. Bracketed values are estimated seasonal actual ET (ETa) differences in mm. This table is a partial summary of graphical data presented in Figure 12.

Differencing Years	Helmand1 (upstream)	Helmand2 (downstream)	Helmand3 (downstream)
2001-2000	Decrease (-56)	Increase (+52)	Increase (+117)
2002-2001	Increase (+89)	Decrease (-63)	Decrease (-74)
2003*- anomalous	N/A	N/A	N/A
2006-2005	Decrease (-35)	Increase (+4 mm)	Increase (+51)

*: Since 2003 was an anomalously wet year, we eliminated (N/A) the use of 2003 data for this interpretation (i.e., 2004 minus 2003 and 2003 minus 2002).

Table 3 shows the relative water use variability among the 3 irrigated areas in the Helmand basin with respect to the location of a diversion structure upstream of the town of Lashkar Gah (Figure 13).

The relative water use between the upstream area and the two downstream areas goes in the opposite direction from year to year. For example, when the upstream area (Helmand1) uses less water than the previous year (2000 versus 2001), the downstream areas use more water in the same season and vice-versa. The fact that an increase in water use by the upstream area is met with lower water uses in the downstream areas makes sense from the basic principle of water balance, demonstrating the capability of the model for capturing obvious water use patterns. On the other hand, the model appears to shed light on possible water management scenarios in the Helmand basin where high water use and low water use are alternating on a yearly basis for each of the basins. This could be a deliberate water allocation as regulated by the diversion structure upstream of Lashkar Gah or a process driven by production and market forces. Our speculation is based on the assumption that, for example, if the upstream basin produces well in one year, they may not need to produce as much the following year.
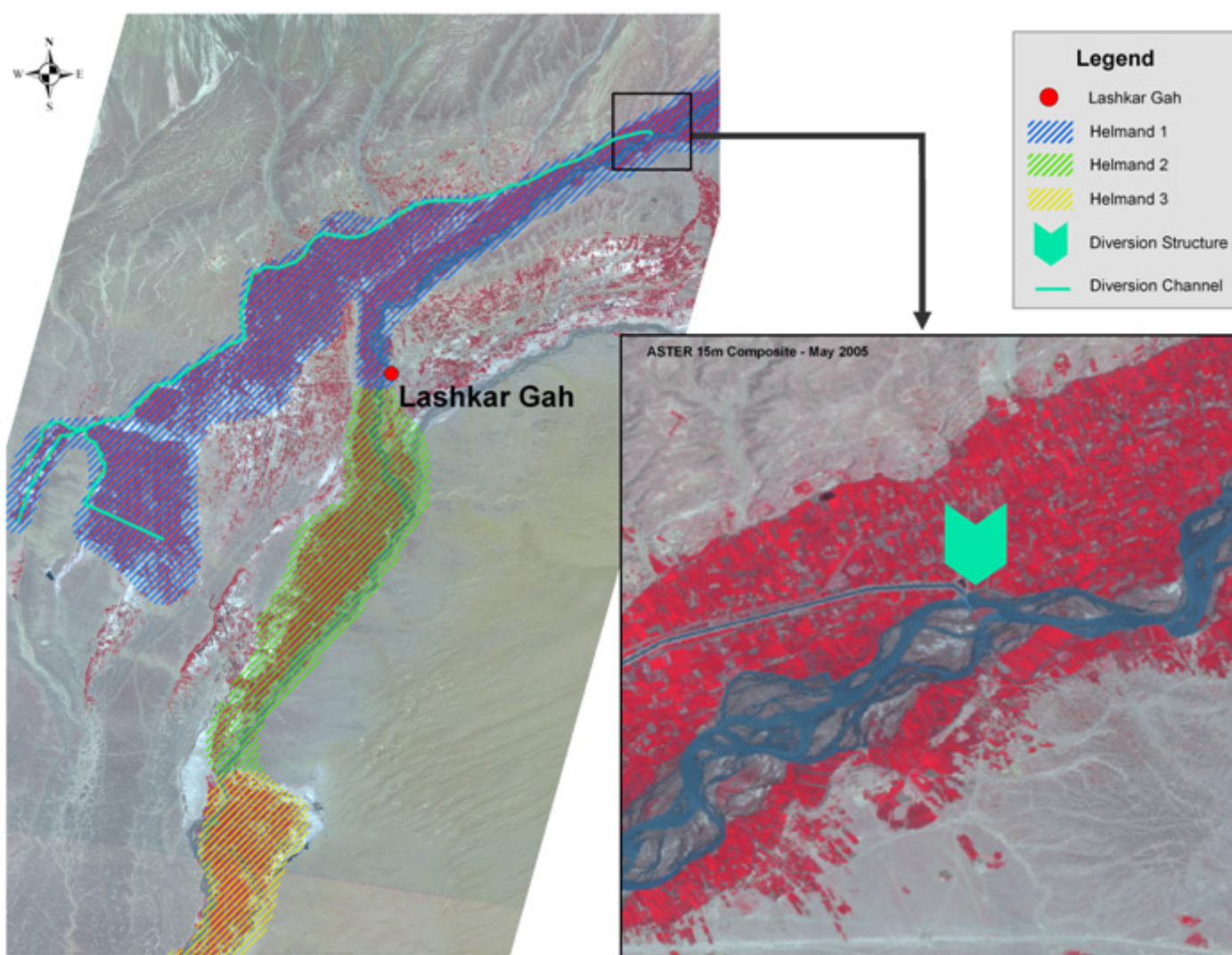

Figure 13. Location of a diversion structure on the Helmand River upstream of Lashkar Gah. The diversion channel is visible in the enlarged portion of the 15-m ASTER image above (right). The extent of the channel runs along the northern section of the Helmand 1 area, west of Lashkar Gah, and is highlighted in the image on the left.

4. Discussion

Although the simplified surface energy balance (SSEB) approach has produced convincing results with encouraging comparisons with other established energy balance models, the model needs to be validated using actual field data. Further comparison with other more robust models will help identify its limitations and potential for different regions. Due to the prohibitive nature of collecting field data in this region of the world, we lack a good measure against which to validate our results. However, a recent comparison with the SEBAL model using Landsat Thermal data in China produced promising results with a coefficient of determination (R^2) of 0.89 (Cai Xueliang, 2007, personal communication). Figure 5 shows a similar comparison work in the US with the METRIC and SEBAL models where strong correlations have been exhibited. The authors intend to carry out a more detailed validation of the model in the United States using a combination of field measurements and results from water balance and other energy balance models. Currently, the model is appropriate to apply in a relatively homogeneous landscape where surface temperature variation is primarily caused by differences in water use. Therefore, major differences due to elevation, aspect, latitude, etc., should be taken into consideration before applying the method on the entire landscape. Furthermore, this method is somehow optimized to estimate actual ET (ETa) on crop surfaces since the albedo magnitude (0.23) embedded in the ETo is based on the grass reference ET. This is, however, a lesser problem than differences in elevation. Future improvement of the model will plan to take into account difference in albedo from other land cover types so that the model can be applied irrespective of land cover. In addition, the model may provide a high end estimate of the seasonal ET because it assumes the presence of well-watered, full-canopy, actively-growing vegetation during the early and late season of the crop cycle for the cold pixel. Again, further refinements of the model will include the use of NDVI to correct for vegetation cover condition to better estimate the actual ET at the wet pixel, based on a recommendation from Rick Allen (personal communication, 2006). Since an accurate estimation of the bare soil evaporation (Hot pixel) requires a water balance method, an integrated modeling framework that couples SSEB with a water-balance-based landscape ET model (VegET) is being developed at the Geographic Information Science Center of Excellence (GIScCE), a joint collaborative center between USGS/EROS and South Dakota State University.

5. Conclusions

The main objective of this study was achieved with the demonstration of the successful coupling of remotely sensed data and a simplified surface energy balance (SSEB) approach in producing estimates actual ET in irrigated agricultural areas of the Kabul and Helmand basins in Afghanistan. The ET fractions are comparable to the commonly used crop coefficient (Kc) (with a soil water stress factor, Ks) and thus are directly multiplied with ETo values to obtain actual ET estimates. A major advantage of the energy-balance approach is that it can be used to quantify spatial extent of irrigated fields and their water-use dynamics without a reference to source of water as opposed to a water-balance model which requires knowledge of both the magnitude and temporal distribution of rainfall and irrigation applied to fields.

The actual ET values of the irrigated fields in the study area varied from year to year in a way that was consistent with field reports and other independent data sets such as the seasonal maximum NDVI

and output from an irrigation supply/demand water balance model. The 2003 seasonal actual ET of the study area was much higher than the rest of the studied years, and about 20 percent higher than the average of the 5 years. This was in agreement with published reports [14] and news sources stating that 2003 precipitation appeared to have broken the sequence of preceding consecutive dry years in Afghanistan.

A close examination of the spatial distribution of the actual ET estimates during the six years revealed that the reduction in area of high actual ET values during less intense water use years was primarily in an area further from the main stream channels. Because this corresponds to a common practice in which water is generally used first by those upstream, the result reinforces the reliability of this approach and points to the potential application of this method for spatially estimating cropped area in irrigated fields. The method also captured probable water management scenarios where a unique year-to-year variability was identified in addition to water use difference between upstream and downstream areas. The existence of a variable temporal pattern between the *hot* and *cold* pixels during the crop season is also believed to be potentially useful in detecting time of start of season for crop monitoring activities. However, further examination of the relationship between time series of ETa and NDVI is needed.

Although the results obtained from the thermal-based ET fraction approach in SSEB are encouraging for applications in remote locations where field-based information is not readily available, it is recommended that the method needs to be further investigated and validated using more detailed surface energy balance methods and field data under different hydro-climatic conditions.

References

1. Senay, G.B. and J. Verdin. Characterization of Yield Reduction in Ethiopia Using a GIS-Based Crop Water Balance Model. *Canadian Journal of Remote Sensing* **2003**, 29(6):687-692.

2. Verdin, J. and R. Klaver. Grid cell based crop water accounting for the famine early warning system. *Hydrological Processes* **2002**, 16: 1617-1630.

3. Allen, R.G., M. Tasurmi, A.T. Morse, R. Trezza. A Landsat-based Energy Balance and Evapotranspiration Model in Western US Water Rights Regulation and Planning. *Journal of Irrigation and Drainage Systems* **2005**, 19 (3-4): 251-268(18)

4. Bastiaanssen, W.G.M., M. Menenti, R.A. Feddes, A.A.M. Holtslag. A remote sensing surface energy balance algorithm for land (SEBAL): 1) Formulation. *Journal of Hydrology* **1998**, 212 (213):213-229.

5. Bastiaanssen, W.G.M. SEBAL-based sensible and latent heat fluxes in the   irrigated Gediz Basin, Turkey. *Journal of Hydrology* **2000**, 229:87-100.

6. Bastiaanssen, W.G.M., E.J.M. Noordman, H. Pelgrum, G. Davids, B.P. Thoreson and R.G. Allen. SEBALmodel with remotely sensed data to improve water resources management under actual field conditions. *Journal of irrigation and drainage engineering* **2005**, 131 (1):85-93.

7. Su, H., M.F. McCabe, E. F. Wood, Z. Su and J. Prueger. Modeling evapotranspiration during SMACEX: comparing two approaches for local and regional scale prediction. *Journal of Hydrometeorology 2005*, 6(6): 910-922.

8. Sadler, E. J., P. J. Bauer, W.J. Busscher and J. A. Millen**.** Site-specific analysis of a droughted corn crop: water use and stress. *Agronomy Journal* **2000**, 92:403-410.

9. Jackson, R.D. Canopy temperature and crop water stress. *Vol 1. Advances in irrigation.* Academic Press, New York, **1982**; pp 43-85.

10. Qiu, G. Y., K. Miyamoto, S. Sase and L. Okushima. Detection of Crop Transpiration and Water Stress by Temperature Related Approach Under Field and Greenhouse Conditions. Department of Land Improvement, National Research Institute of Agricultural Engineering, Tsukuba, Ibraki, Japan, **1999**.

11. Senay, G.B. and J. Verdin. Evaluating reference evapotranspiration (ETo) model output from the Global Data Assimilation System using station ETo in the US. Proceedings of Reclamation ET workshop: state-of-the-art review of ET remote sensing science and technology, Feb 8-10, **2005**; Fort Collins, Colorado.

12. Allen, R.G., L. Pereira, D. Raes, and M. Smith. Crop Evapotranspiration. Food and Agriculture Organization of the United Nations, Rome, Italy, **1998**; ISBN 92-5-104219-5. 290p.

13. ESRI. ArcGIS 9.0. Environmental Systems Research Institute (ESRI). Redlands, CA. **2004.**

14. FEWS NET. Afghanistan Monthly Food Security Bulletin. September**, 2003**. (www.fews.net)

15. Doorenbos, J. and W.O. Pruitt. Crop water requirements. FAO Irrigation and Drainage Paper No. 24. Food and Agricultural Organization of the United Nations, Rome, Italy, **1977**; 144p.

Note: any mention of trade, product, or firm names is for descriptive purposes only and does not imply endorsement by the U.S. Government.